Математички Билтен
49 (LXXV) 1 (2025), 55–74

UDC: ???
DOI: ???

A UNIFORMLY CONVERGENT METHOD FOR A LINEAR SINGULARLY–PERTURBED REACTION–DIFFUSION PROBLEM ON A LISEIKIN TYPE OF MESH

SAMIR KARASULJIĆ [1]

Abstract. In this paper, we consider the numerical solution of a linear singularly perturbed reaction-diffusion boundary value problem, where a small perturbation parameter multiplies the second-order derivative. To achieve this, we approximate the differential equation using a central difference scheme on a Liseikin-type mesh. Furthermore, it is shown that the proposed method is uniformly convergent with respect to the perturbation parameter with an order of convergence of 2. Finally, we provide two numerical examples that illustrate the theoretical results regarding the uniform convergence of the discrete problem, as well as the robustness of the method.

1. INTRODUCTION

Consider the following reaction-diffusion problem: find $u \in C^2(0,1) \cap C[0,1]$ such that

$$-\varepsilon^2 u'' + c(x)u + f(x) = 0, \quad x \in (0,1), \quad u(0) = A,\ u(1) = B, \tag{1.1}$$

under the condition

$$c(x) \geqslant \gamma^2 > 0, \quad x \in [0,1], \tag{1.2}$$

where $\varepsilon \in (0,1]$ is a small perturbation parameter. If $c, f \in C[0,1]$, then, according to [11], there exists a unique solution $u \in C^2[0,1]$ to problem (1.1) under condition (1.2).

Differential equations are said to be singularly perturbed if they contain a small parameter ε that multiplies the highest-order derivative. Such equations

2010 *Mathematics Subject Classification.* Primary: 65L10, 65L11, 65L50.

Key words and phrases. Singular perturbation, reaction–diffusion, boundary layer, Liseikin mesh, layer-adapted mesh, uniform convergence.

frequently occur in the description of various phenomena in engineering, natural sciences, economics, and sociology. The exact solutions of these equations are characterized by the appearance of layers where the solution changes rapidly.

The exact solution to this problem exhibits rapid changes in the vicinity of the endpoints $x = 0$ and $x = 1$ as the perturbation parameter ε tends to zero. The issue lies in the fact that standard numerical methods, which do not account for the characteristics of the exact solution, are incapable of resolving these layers. The performance of such methods deteriorates as ε approaches zero. Consequently, the numerical solution becomes unreliable in this case, as the magnitude of the error is deemed unacceptable. To overcome this, methods that are uniformly convergent with respect to the perturbation parameter ε are required. Numerical methods are said to be ε-uniformly convergent if they demonstrate uniform behavior for all values of the singular perturbation parameter.

The most prevalent approach for constructing such methods is the utilization of fitted meshes, also referred to as layer-adapted or layer-resolving meshes. Bakhvalov [1] was the first to construct meshes specifically for solving singularly perturbed problems. Bakhvalov-type meshes necessitate detailed information about the solution; they are uniformly spaced outside the layers and are characterized by a gradual transition from a coarse to a very fine mesh within the layers. Another approach involves piecewise equidistant meshes, as introduced by Shishkin [14, 15]. The construction of these meshes is very simple: Shishkin joins fine and coarse meshes at a carefully chosen transition point.

In this paper, we employ the mesh developed by Liseikin [8, 10, 6, 7, 9], which has demonstrated excellent capabilities in resolving not only exponential layers but also other layer types. Many authors have contributed to research on problems (1.1)–(1.2) and similar problems. To avoid listing all authors individually, details of these results can be found in the monographs [5, 12, 4, 13] and the references therein.

Remark 1.1: Throughout this paper, we let C, sometimes subscripted, denote a generic positive constant that may take different values in different formulas but is always independent of N and ε.

2. Properties of the exact solution and layer–adapted meshes

Information regarding the behavior of the exact solution and its derivatives, particularly within the layers, is a critical component in the construction of layer-adapted meshes. This information is necessary not only for the mesh construction but also for the convergence analysis of the numerical method. The following theorem provides the estimates required for the subsequent sections of this paper.

Theorem 1. [5] *Let $c, f \in C^4[0,1]$. Then*

$$\left|u^{(p)}(x)\right| \leqslant C\left\{1+\varepsilon^{-p}e^{-\gamma x/\varepsilon}+\varepsilon^{-p}e^{-\gamma(1-x)/\varepsilon}\right\}, \text{ for } x\in(0,1),\ p=0,1,\ldots,4. \tag{2.1}$$

Furthermore, the solution u to problem (1.1)–(1.2) *can be decomposed as $u = r + l_0 + l_1$. For $p = 0, 1, \ldots, 4$, the regular component r satisfies $\|r^{(p)}\|_\infty \leqslant C$, while for the layer*

components l_0 and l_1, we have

$$\left|l_0^{(p)}(x)\right| \leqslant C\varepsilon^{-p}e^{-\gamma x/\varepsilon}, \quad \left|l_1^{(p)}(x)\right| \leqslant C\varepsilon^{-p}e^{-\gamma(1-x)/\varepsilon}, \quad x \in [0,1].$$

In constructing our numerical method, we utilize a layer-adapted mesh introduced by Liseikin [7, p. 232]. Liseikin developed a mesh transformation function, denoted by x_L, which maps equidistant meshes onto layer-adapted meshes. This function resolves the layer in the vicinity of the endpoint $x = 0$ and is defined as follows:

$$x_L(\xi,\varepsilon,a,k) = \begin{cases} c_1\varepsilon^k\left[(1-d\xi)^{-1/a}-1\right], & 0 \leqslant \xi \leqslant \xi_0 \\ c_1\left[\varepsilon^{k(1-\beta/a)} - \varepsilon^k + \left(\frac{\varepsilon^k}{(1-d\xi)^{1/a}}\right)'(\xi_0)(\xi-\xi_0)\right. \\ +\frac{1}{2}\left(\frac{\varepsilon^k}{(1-d\xi)^{1/a}}\right)''(\xi_0)(\xi-\xi_0)^2 + \ldots + \\ \left. + \frac{1}{l!}\left(\frac{\varepsilon^k}{(1-d\xi)^{1/a}}\right)^{(l)}(\xi_0)(\xi-\xi_0)^l + c_0(\xi-\xi_0)^{l+1}\right], & \xi_0 < \xi \leqslant m_1, \end{cases} \tag{2.2}$$

where $l \leq n$, $d = (1-\varepsilon^{k\beta})/\xi_0 \geq 1 + m_1 > 1$, $\beta = a/(1+na)$, $1-\beta/a = na/(1+na)$, and $c_0 \geq 0$. Here, a is an arbitrary positive constant such that $a \geq m_2 > 0$, and c_1 is chosen to satisfy the boundary condition $x_L(1,\varepsilon,a,k) = 1$. The parameter k represents the scale of the layer; for the problem considered here, we set $k = 1$.

To satisfy our criteria, it is sufficient to set $l = 2$, yielding the coordinate transformation also provided in [7, p. 232]:

$$x_{L1}(\xi,\varepsilon,a,k) = \begin{cases} c_1\varepsilon^k\left[(1-d\xi)^{-1/a}-1\right], & 0 \leqslant \xi \leqslant \xi_0, \\ c_1[\varepsilon^{kan/(1+na)} - \varepsilon^k + \dfrac{d}{a}\varepsilon^{ka(n-1)/(1+na)}(\xi-\xi_0) \\ +\dfrac{d^2}{2a}\left(\dfrac{1}{a}+1\right)\varepsilon^{ka(n-2)/(1+na)}(\xi-\xi_0)^2 \\ +c_0(\xi-\xi_0)^3], & \xi_0 < \xi \leqslant m_1. \end{cases} \tag{2.3}$$

As previously mentioned, the coordinate transformation (2.3) is specifically designed to resolve the boundary layer near $x = 0$. However, the solution to (1.1) exhibits two boundary layers, located at the endpoints $x = 0$ and $x = 1$. Consequently, the transformation (2.3) must be modified to effectively capture both layers. This can be achieved in the following way:

$$x(\xi,\varepsilon,a,k) = \begin{cases} x_{L1}(\xi,\varepsilon,a,k), & 0 \leqslant \xi \leq 1/2, \\ 1 - x_{L1}(1-\xi,\varepsilon,a,k), & 1/2 < \xi \leqslant 1. \end{cases} \tag{2.4}$$

The constant c_1 can be determined from the condition $x_{L1}(1/2,\varepsilon,a,1) = 1/2$, which yields:

$$c_1 = 1/\left[2\varepsilon^{an/(1+na)} - 2\varepsilon + \frac{d}{a}\varepsilon^{a(n-1)/(1+na)} + \frac{d^2}{4a}\left(\frac{1}{a}+1\right)\varepsilon^{a(n-2)/(1+na)} + \frac{c_0}{4}\right].$$

The coordinate transformation (2.4) divides the interval $[0,1]$ into three subintervals: $[0, x(\xi_0,\varepsilon,a,1)]$, $[x(\xi_0,\varepsilon,a,1), 1-x(\xi_0,\varepsilon,a,1)]$, and $[1-x(\xi_0,\varepsilon,a,1),1]$. For the subsequent analysis, it is sufficient to consider the interval $[0,1/2]$ – specifically, the subintervals $[0,x(\xi_0,\varepsilon,a,1)]$ and $[x(\xi_0,\varepsilon,a,1),1/2]$. On the interval $[0,1/2]$, the layer component l_1 from estimate (2.1) can be omitted since the term $\varepsilon^{-p}e^{-\gamma(1-x)/\varepsilon}$ is negligible. For $x \in [\frac{n\varepsilon}{\gamma}\ln(\varepsilon^{-1}),1/2]$, we have:

$$\left|u^{(p)}(x)\right| \leqslant C\left[1+\varepsilon^{-p}e^{-\frac{\gamma}{\varepsilon}\cdot\frac{n\varepsilon}{\gamma}\ln(\varepsilon^{-1})}\right] = C(1+\varepsilon^{n-p}), \quad 1 \leqslant p \leq n.$$

This inequality implies that the derivatives within the interval $[\frac{n\varepsilon}{\gamma}\ln(\varepsilon^{-1}),1/2]$ are ε-uniformly bounded. By calculating $x(\xi_0,\varepsilon,a,1)$, we obtain:

$$x(\xi_0,\varepsilon,a,1) = c_1\left(\varepsilon^{\frac{na}{1+na}} - \varepsilon\right).$$

Since $x(\xi_0,\varepsilon,a,1) \geqslant \frac{n\varepsilon}{\gamma}\ln(\varepsilon^{-1})$, it follows that the derivatives $u^{(p)}$ for $p \leq n$ are ε-uniformly bounded on the interval $[x(\xi_0,\varepsilon,a,1),1/2]$. Consequently, the remainder of our analysis will focus primarily on the interval $[0,x(\xi_0,\varepsilon,a,1)]$.

We employ the transformation (2.4) to construct the layer-adapted mesh. The interval $[0,1]$ is partitioned by the mesh points $x_i = x(\xi_i,\varepsilon,a,1)$, where $\xi_i = i/N$ for $i = 0,1,\ldots,N$. Note that the points ξ_i form an equidistant mesh on $[0,1]$. Specifically, the layer-adapted mesh is defined as:

$$X_N^h : 0 = x_0 < x_1 < \cdots < x_{N-1} < x_N = 1. \tag{2.5}$$

In the following steps, we denote the mesh step sizes by $h_i = x_i - x_{i-1}$ for $i = 1,2,\ldots,N$.

3. Difference scheme

To obtain a discrete analogue of problem (1.1), we approximate the second derivative u'' at the mesh points x_i for $i = 1,\ldots,N-1$ using the standard central finite difference formula on a non-uniform mesh:

$$u''(x_i) \approx \frac{2}{h_i+h_{i+1}}\left(\frac{u(x_{i+1})-u(x_i)}{h_{i+1}} - \frac{u(x_i)-u(x_{i-1})}{h_i}\right).$$

This leads to the following finite difference scheme:

$$-\frac{2\varepsilon^2}{h_i+h_{i+1}}\left(\frac{u_{i+1}-u_i}{h_{i+1}} - \frac{u_i-u_{i-1}}{h_i}\right) + c(x_i)u_i + f(x_i) = 0, \quad i = 1,\ldots,N-1, \tag{3.1}$$

with the boundary conditions $u_0 = A$ and $u_N = B$, where $u^h = (u_0,u_1,\ldots,u_N)$ is the numerical solution to be calculated. Based on the difference scheme (3.1), we

define the discrete operator L_i^h as follows:

$$L_i^h[u^h] \equiv -\frac{2\varepsilon^2}{h_i + h_{i+1}} \left(\frac{u_{i+1} - u_i}{h_{i+1}} - \frac{u_i - u_{i-1}}{h_i} \right) + c(x_i)u_i + f(x_i), \quad i = 1, \ldots, N-1, \tag{3.2}$$

$$\mathcal{G}^h[u^h] \equiv (u_0, u_N) = (A, B). \tag{3.3}$$

4. Uniform convergence

Solving the discrete problem

$$L_i^h[u^h] = 0, \quad i = 1, \ldots, N-1, \tag{4.1}$$

$$\mathcal{G}^h[u^h] = (u_0, u_N) = (A, B), \tag{4.2}$$

yields the numerical solution $u^h = (u_0, u_1, \ldots, u_N)$. We now investigate the error $r_i = u_i - u(x_i)$ for $i = 0, 1, \ldots, N$. The main result regarding the error is provided in the convergence theorem. Before stating and proving the theorem, we establish a lemma regarding several terms that appear in the convergence analysis.

Lemma 1. *Let h_i, $i = 1, \ldots, N$, be the step sizes of mesh* (2.5)*, and let u''' and $u^{(4)}$ denote the derivatives of the exact solution to problem* (1.1)–(1.2)*. Then, the following estimates hold:*

$$\left| \varepsilon^2 (h_{i+1} - h_i) u'''(x_i) \right| \leqslant \frac{C}{N^2} \quad \textit{and} \quad \left| \frac{\varepsilon^2}{h_i + h_{i+1}} \left[u^{(4)}(\mu_i^+) h_{i+1}^3 + u^{(4)}(\mu_i^-) h_i^3 \right] \right| \leqslant \frac{C}{N^2}, \tag{4.3}$$

for $i = 1, 2, \ldots, N-1$, where $\mu_i^- \in (x_{i-1}, x_i)$ and $\mu_i^+ \in (x_i, x_{i+1})$.

Proof. We begin by deriving the following estimates. For $x \in [0, x(\xi_0, \varepsilon, a, 1)]$, we have:

$$\begin{aligned} \left| u'(x) x'(\xi) \right| &\leqslant C \left| \left(1 + \varepsilon^{-1} e^{-\frac{\gamma}{\varepsilon} \cdot c_1 \varepsilon [(1 - d\xi)^{-1/a} - 1]} \right) \cdot c_1 \varepsilon (1 - d\xi)^{-1/a - 1} \right| \\ &\leqslant C c_1 \left(\varepsilon (1 - d\xi)^{-1/a - 1} + \frac{e^{-\gamma c_1 [(1 - d\xi)^{-1/a} - 1]}}{(1 - d\xi)^{1/a + 1}} \right) \leqslant C_1. \end{aligned} \tag{4.4}$$

From Theorem 1 and the calculation of the first derivative of $x(\xi)$ for $\xi \in [0, \xi_0]$, neglecting the term $\varepsilon^{-2} e^{-\gamma(1-x)/\varepsilon}$, we obtain the following inequality:

$$\begin{aligned} \left| u''(x) \left(x'(\xi) \right)^2 \right| &\leqslant C \left(1 + \varepsilon^{-2} e^{-\gamma x/\varepsilon} \right) \left[\frac{c_1 \varepsilon d}{a} \left(1 - d\xi \right)^{-1/a - 1} \right]^2 \\ &= C \left(1 + \varepsilon^{-2} e^{-\gamma c_1 \left[(1 - d\xi)^{-1/a} - 1 \right]} \right) \left[\frac{c_1 \varepsilon d}{a} \left(1 - d\xi \right)^{-1/a - 1} \right]^2 \\ &= \frac{C c_1^2 d^2}{a^2} \cdot \frac{\varepsilon^2}{(1 - d\xi)^{2/a + 2}} + \frac{C c_1^2 d^2 e^{\gamma c_1}}{a^2} \cdot \frac{e^{-\gamma c_1 (1 - d\xi)^{-1/a}}}{(1 - d\xi)^{2/a + 2}}. \end{aligned}$$

The term $\frac{\varepsilon^2}{(1-d\xi)^{2/a+2}}$ attains its maximum at $\xi = \xi_0$. Substituting $\xi = \xi_0$ and $d = \frac{1-\varepsilon^{a/(1+na)}}{\xi_0}$ into this expression, we obtain:

$$\frac{\varepsilon^2}{(1-d\xi)^{2/a+2}} = \frac{\varepsilon^2}{\varepsilon^{\frac{a}{1+na}\cdot\frac{2+2a}{a}}} = \varepsilon^{\frac{2a(n-1)}{1+na}} < C,$$

since $n = 4$. To estimate the term $\frac{e^{-\gamma c_1(1-d\xi)^{-1/a}}}{(1-d\xi)^{2/a+2}}$, we consider the function $x \mapsto \frac{e^{-\gamma c_1 x^{-1/a}}}{x^{2/a+2}}$. By applying L'Hôpital's rule five times to the limit $\lim_{x\to 0_+} \frac{x^{-\frac{2}{a}-2}}{e^{\frac{\gamma c_1}{x^{1/a}}}}$, we have:

$$\lim_{x\to 0_+} \frac{x^{-\frac{2}{a}-2}}{e^{\frac{\gamma c_1}{x^{1/a}}}} = \frac{8a(a+1)(2a+1)(2a-1)(a-1)}{\gamma^5 c_1^5} \lim_{x\to 0_+} \frac{x^{\frac{3}{a}-2}}{e^{\frac{\gamma c_1}{x^{1/a}}}} = 0,$$

for $a < \frac{3}{2}$. Each subsequent application of L'Hôpital's rule increases the range of the parameter a by $1/2$ for which the limit remains zero. Next, we examine the first derivative of the function $x \mapsto \frac{e^{-\gamma c_1 x^{-1/a}}}{x^{2/a+2}}$:

$$\left(\frac{e^{-\gamma c_1 x^{-1/a}}}{x^{2/a+2}}\right)' = \frac{e^{-\gamma c_1 x^{-1/a}} \left[\frac{\gamma c_1}{a} - \left(\frac{2}{a}+2\right) x^{1/a}\right]}{x^{3/a+3}}.$$

This derivative vanishes at $x = \left(\frac{\gamma c_1}{2(a+1)}\right)^a$. Considering the sign of the derivative, we conclude that the function has a local maximum at this point. The value of the function at the maximum is $\frac{e^{-2(a+1)}}{\left(\frac{\gamma c_1}{2(a+1)}\right)^{2a+2}}$.Based on the preceding analysis, we conclude that the following inequality holds:

$$\left|u''(x)(x'(\xi))^2\right| \leq C_1. \tag{4.5}$$

The mesh step sizes h_i satisfy

$$h_i = \int_{\xi_{i-1}}^{\xi_i} x'(t)\mathrm{d}t \quad \text{and} \quad |h_{i+1} - h_i| = \left|\int_{\xi_{i-1}}^{\xi_i} \int_t^{t+1/N} x''(s)\mathrm{d}s\mathrm{d}t\right|. \tag{4.6}$$

Furthermore, we have

$$h_i \leq |x'(\zeta_i)|\frac{1}{N} \quad \text{and} \quad |h_{i+1} - h_i| \leq |x''(\nu_i)|\frac{1}{N^2}, \tag{4.7}$$

where $\zeta_i \in (\xi_{i-1}, \xi_i)$, $\nu_i \in (\xi_{i-1}, \xi_{i+1})$, and $1/N = \xi_i - \xi_{i-1}$ for $i = 1, \ldots, N$. Consequently, it holds that

$$\begin{aligned}\left|\frac{\varepsilon^2(h_{i+1}-h_i)}{3}u'''(x_i)\right| \\ \leqslant C\left|u'(x_i)(h_{i+1}-h_i)\right| \leqslant C\left|u'(x_i)x''(\nu_i)\frac{1}{N^2}\right| \leqslant \frac{C}{N^2}.\end{aligned} \tag{4.8}$$

According to Theorem 1, we have:

$$\left|u^{(4)}(x)\right| \leqslant C_1 \left[1 + \varepsilon^{-4} e^{-\gamma x/\varepsilon} + \varepsilon^{-4} e^{-\gamma(1-x)/\varepsilon}\right],$$
$$\left|u''(x)\right| \leqslant C_2 \left[1 + \varepsilon^{-2} e^{-\gamma x/\varepsilon} + \varepsilon^{-2} e^{-\gamma(1-x)/\varepsilon}\right],$$

and these inequalities imply that

$$\varepsilon^2 \left|u^{(4)}(x)\right| \leq C_3 \left|u''(x)\right|.$$

Now, using this relation and inequality (4.5), we obtain:

$$\begin{aligned}
&\frac{\varepsilon^2}{h_i + h_{i+1}} \left|u^{(4)}(\mu_i^+) h_{i+1}^3 + u^{(4)}(\mu_i^-) h_i^3\right| \\
&\qquad = \varepsilon^2 \left|u^{(4)}(\mu_i^+)\right| h_{i+1}^2 \frac{h_{i+1}}{h_i + h_{i+1}} + \varepsilon^2 \left|u^{(4)}(\mu_i^-)\right| h_i^2 \frac{h_i}{h_i + h_{i+1}} \\
&\qquad \leqslant C_1 \left(\left|u''(\mu_i^+)\right| h_{i+1}^2 + \left|u''(\mu_i^-)\right| h_i^2\right) \\
&\qquad \leqslant C_1 \left[\left|u''(\mu_i^+)\right| \left(\int_{\xi_i}^{\xi_{i+1}} x'(t)\,\mathrm{d}\,t\right)^2 + \left|u''(\mu_i^-)\right| \left(\int_{\xi_{i-1}}^{\xi_i} x'(t)\,\mathrm{d}\,t\right)^2\right] \\
&\qquad \leqslant C_1 \left(\left|u''(\mu_i^+)\right| \left(x'(\nu_i^+)\right)^2 \frac{1}{N^2} + \left|u''(\mu_i^-)\right| \left(x'(\nu_i^-)\right)^2 \frac{1}{N^2}\right) \\
&\qquad \leqslant \frac{C}{N^2},
\end{aligned} \tag{4.9}$$

where $\mu_i^+ \in (x_i, x_{i+1})$, $\mu_i^- \in (x_{i-1}, x_i)$, $\nu_i^+ \in (\xi_i, \xi_{i+1})$, and $\nu_i^- \in (\xi_{i-1}, \xi_i)$.

Taking into account that the derivatives are ε–uniformly bounded on the interval $[x(\xi_0, \varepsilon, a, 1), 1/2]$, and the inequalities (4.8), (4.9), the lemma is proven.

□

We define a barrier function based on the quadratic $x \mapsto -x^2 + x + D$, where the constant D is chosen such that the function satisfies two primary conditions: first, $x \mapsto -x^2 + x + D$ must be positive on $[0, 1]$, and second, its second derivative must be negative on $(0, 1)$, as illustrated in Figure 1. A third condition will be specified within the convergence theorem.

In order to estimate the error of the difference scheme (3.1), we introduce the operator:

$$\mathbf{L}_u^h = \{L_{i\mathbf{u}}^h\}, \quad i = 1, 2, \ldots, N-1,$$
$$Ł_{i\mathbf{u}}^h[\mathbf{v}] \equiv L_i^h[\mathbf{u} + \mathbf{v}] - L_i^h[\mathbf{u}],$$

where $\mathbf{v} = (v_0, v_1, \ldots, v_N)$ and $\mathbf{u} = (u(x_0), u(x_1), \ldots, u(x_N))$, with $u(x)$ being the solution to problem (1.1)–(1.2).

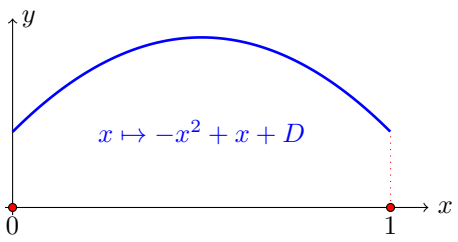

FIGURE 1. The function $x \mapsto -x^2 + x + D$.

Let $\mathbf{r} = \{r_i\} = \{u_i^h - u(x_i)\}$, for $i = 0, 1, \ldots, N$, denote the error vector, where $\mathbf{u}^h$ is the solution to the discrete problem (4.1)–(4.2). It then follows that:

$$L_{i\mathbf{u}}^h[\mathbf{r}] = R_i, \quad i = 1, 2, \ldots, N-1, \tag{4.10}$$

where R_i represents the truncation error of the approximation (4.1)–(4.2) at the mesh point x_i.
The main result is presented in the following convergence theorem.

Theorem 2. *Let u be the exact solution to problem* (1.1)–(1.2). *Then, the following estimate holds:*

$$|u(x_i) - u_i| \leqslant \frac{C}{N^2}, \quad i = 0, 1, \ldots, N,$$

where u_i is the value of the numerical solution u^h at the mesh point x_i, obtained by the discrete problem (3.2) *on the grid* (2.5) *generated by the transformation function* (2.4).

Proof. To estimate the error vector $\mathbf{r} = (r_0, r_1, \ldots, r_N)$, where $r_i = u(x_i) - u_i$ for $i = 0, 1, \ldots, N$, we first evaluate $L_{i\mathbf{u}}^h[\mathbf{r}]$. It holds that:

$$L_{i\mathbf{u}}^h[\mathbf{r}] = -\frac{\varepsilon^2(h_{i+1} - h_i)}{3} u'''(x_i) - \frac{\varepsilon^2}{12(h_i + h_{i+1})} \left[u^{(4)}(\mu_i^+) h_{i+1}^3 + u^{(4)}(\mu_i^-) h_i^3 \right], \tag{4.11}$$

for $i = 1, \ldots, N-1$, where $\mu_i^- \in (x_{i-1}, x_i)$ and $\mu_i^+ \in (x_i, x_{i+1})$. According to the notation in (4.10) and Lemma 1, the following estimates are valid:

$$|R_i| \leqslant \frac{C}{N^2}, \quad i = 1, 2, \ldots, N-1, \tag{4.12}$$

which implies:

$$\max_{1 \leqslant i \leqslant N-1} |R_i| \leqslant \frac{C}{N^2}. \tag{4.13}$$

We now define a discrete barrier function $\mathbf{g} = (g_0, g_1, \ldots, g_N)$ as:

$$g_i = C_1(-x_i^2 + x_i + D) \max_{1 \leqslant i \leqslant N-1} |R_i|.$$

The third condition for the constant D is to ensure that:

$$-g_0 \leqslant r_0 \leqslant g_0 \quad \text{and} \quad -g_N \leqslant r_N \leqslant g_N. \tag{4.14}$$

This is readily satisfied since $r_0 = u(0) - u_0 = 0$ and $r_N = u(1) - u_N = 0$.

Calculating $L^h_{i\mathbf{u}}[\mathbf{g}]$, we obtain:

$$L^h_{i\mathbf{u}}[\mathbf{g}] = C_1 \max_{1\leqslant i\leqslant N-1} |R_i| \left[2\varepsilon^2 + c(x_i)(-x_i^2 + x_i + D)\right]. \tag{4.15}$$

By choosing C_1 sufficiently large and considering condition (1.2), we arrive at:

$$L^h_{i\mathbf{u}}[-\mathbf{g}] \leqslant L^h_{i\mathbf{u}}[\mathbf{r}] \leq L^h_{i\mathbf{u}}[\mathbf{g}], \quad i = 1, 2, \ldots, N-1. \tag{4.16}$$

Combined with the boundary estimates (4.14), and taking into account the discrete maximum principle, this yields:

$$|r_i| \leqslant g_i, \quad i = 0, 1, \ldots, N.$$

Consequently, we conclude that:

$$|u(x_i) - u_i| \leqslant \frac{C}{N^2}, \quad i = 0, 1, \ldots, N,$$

which completes the proof. □

5. Numerical experiments

In this section, we conduct several numerical experiments to validate the proposed method and confirm the theoretical results. These results are obtained by solving the discrete problem (4.1)–(4.2) on the non-uniform mesh (2.5). Two test problems are considered. For the first problem, the exact solution is known, whereas for the second problem, it is unknown. All computations are performed for various values of the perturbation parameter ε and the number of mesh points N. Specifically, the parameter ε ranges from 2^{-1} to 2^{-40}, and N varies from 2^5 to 2^{12}.

As is well known, Bakhvalov- and Shishkin-type meshes, as well as their modifications, are specifically constructed to solve problems exhibiting exponential layers. Consequently, these two meshes are included in our numerical experiments to provide a comparison with the results obtained using the Liseikin mesh. We adopt the notation from [3], supplemented by the indices "B" and "Sh" to denote the respective mesh types. The generating function for the Bakhvalov mesh is given by:

$$x_B(\xi) = \begin{cases} \varphi(\xi) := a_B \varepsilon \ln \frac{q_B}{q_B - \xi}, \ \xi \in [0, \alpha_B], \\ \varphi(\alpha_B) + \varphi'(\alpha_B)(\xi - \alpha_B), \ \xi \in [\alpha_B, 0.5], \\ 1 - x_B(1 - \xi), \ \xi \in [0.5, 1], \end{cases} \tag{5.1}$$

where a_B and q_B are constants independent of ε such that $q_B \in (0, 0.5)$ and $\alpha_B \in (0, q_B/\varepsilon)$, and additionally $a_B\gamma \geqslant 2$.

The generating function for the Shishkin mesh is defined as:

$$x_{Sh}(\xi) = \begin{cases} 4\alpha_{Sh}\xi, \ \xi \in [0, \alpha_{Sh}], \\ \alpha_{Sh} + 2(1 - 2\alpha_{Sh})(\xi - 0.25), \ \xi \in [\alpha_{Sh}, 0.5], \\ 1 - x_{Sh}(1 - \xi), \ \xi \in [0.5, 1], \end{cases} \tag{5.2}$$

with

$$\alpha_{Sh} = \min\{1/4,\ 4\gamma_0^{-1}\varepsilon \ln N\}, \quad \gamma_0 = \min\{\gamma, 1\}.$$

To demonstrate the robustness and efficiency of the proposed method using grids generated by (2.5) and (5.1) (i.e., the Liseikin and Bakhvalov meshes), we compute the maximum nodal error E_N and the numerical rate of convergence Ord. When the exact solution $u(x)$ to problem (1.1)–(1.2) is known, the error is calculated as:

$$E_N = \max_{0\leqslant i\leqslant N} |u(x_i) - u_{N,i}|.$$

Here, $u(x_i)$ represents the value of the exact solution at the mesh point x_i. In cases where the exact solution is unknown, we use the formula:

$$E_N = \max_{0\leqslant i\leqslant N} |u_{2N,2i} - u_{N,i}|,$$

where $u_{N,i}$ denotes the value of the numerical solution obtained on a mesh with N intervals at the mesh points x_i, and $u_{2N,2i}$ is the value of the numerical solution on a mesh with $2N$ intervals evaluated at the same points. The rate of convergence is then estimated by:

$$\text{Ord} = \frac{\ln(E_N) - \ln(E_{2N})}{\ln 2}.$$

When using the Shishkin mesh with a known exact solution to problem (1.1)–(1.2), the error E_N is calculated in the same manner as for the Liseikin and Bakhvalov meshes. However, if the exact solution is unknown, the error E_N and the rate of convergence Ord are computed using the double-mesh method (see [2]):

$$E_N = \max_{0\leqslant i\leqslant N} |\tilde{u}_{2N,2i} - u_{N,i}|,$$

where $u_{N,i}$ is the value of the numerical solution on a mesh with N subintervals at the mesh point x_i, and $\tilde{u}_{2N,2i}$ is the value of the numerical solution on a mesh with $2N$ subintervals at the same mesh point, where the transition point has been slightly altered to:

$$\tilde{\alpha}_{Sh} = \min\left\{1/4,\ 4\gamma_0^{-1}\varepsilon \ln(N/2)\right\}.$$

This adjustment ensures that the mesh points of the coarse grid coincide with those of the fine grid. In both cases involving the Shishkin mesh (with or without a known exact solution), the numerical rate of convergence is calculated as:

$$\text{Ord} = \frac{\ln E_N - \ln E_{2N}}{\ln \frac{2k}{k+1}}, \quad k = 5, \ldots, 12.$$

Example 1: [16]

Let us consider the following boundary value problem

$$-\varepsilon^2 u'' + u + \cos^2(\pi x) + 2\varepsilon^2\pi^2\cos^2(\pi x) = 0, \quad x \in (0,1),$$

$$u(0) = 0,\ u(1) = 0.$$

The condition (1.2) is fulfilled, because holds $c(x) = 1 > 0$. We know the exact solution to this problem, and that is:

$$u(x) = \frac{e^{-x/\varepsilon} + e^{-(1-x)/\varepsilon}}{1 + e^{-1/\varepsilon}} - \cos^2(\pi x).$$

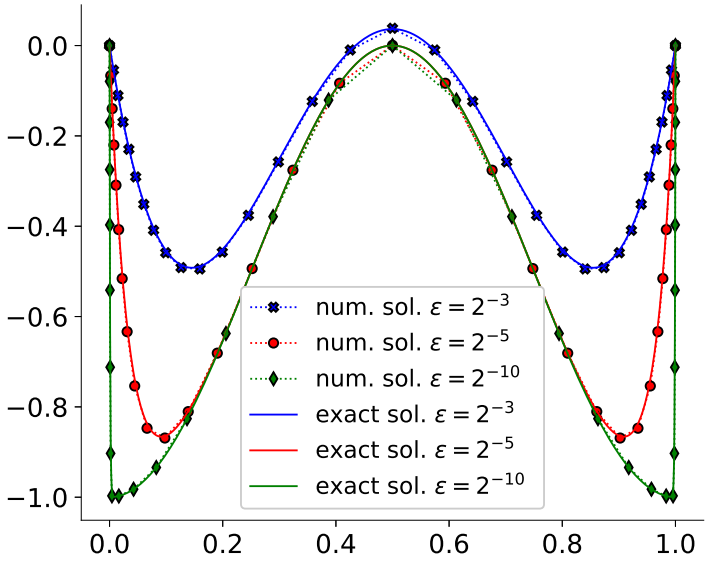

FIGURE 2. The numerical solutions for $N = 32$, the different values of ε on Liseikin mesh, and the exact solutions for the same values of ε.

The obtained results are presented in Figures 2 and 3, and Tables 1, 2, and 3. Figure 2 illustrates the numerical solutions compared to their corresponding exact solutions, computed using the Liseikin mesh for three different values of the parameter ε. Figure 3 provides a detailed view of the numerical solutions within the boundary layer near $x = 0$, where each solution is calculated using a different mesh type. The maximum nodal errors E_N and the numerical rates of convergence Ord are summarized in Tables 1, 2, and 3 for the Liseikin, Bakhvalov, and Shishkin meshes, respectively.

Example 2: Let us consider the following boundary value problem

$$-\varepsilon^2 u'' + (5 + x + e^x)u + x + x^2 - 5 = 0, \quad x \in (0, 1),$$
$$u(0) = 0,\ u(1) = 0.$$

The condition (1.2) is fulfilled, here we have that $c(x) = 5 + x + e^x \geqslant 6 > 0$, $\forall x \in [0, 1]$. The exact solution to this problem is unknown.

Liseikin mesh								
N	E_n	Ord	E_n	Ord	E_n	Ord	E_n	Ord
2^5	2.2872×10^{-3}	2.14	3.0847×10^{-3}	2.03	2.3136×10^{-3}	1.99	2.0345×10^{-3}	1.98
2^6	5.1734×10^{-4}	2.09	7.5064×10^{-4}	2.01	5.8179×10^{-4}	1.99	5.1265×10^{-4}	2.00
2^7	1.2172×10^{-4}	2.04	1.8508×10^{-4}	2.01	1.4551×10^{-4}	1.99	1.2810×10^{-4}	1.99
2^8	2.9452×10^{-5}	2.02	4.5915×10^{-5}	2.00	3.6394×10^{-5}	1.99	3.2046×10^{-5}	2.00
2^9	7.2400×10^{-6}	2.01	1.1432×10^{-5}	2.00	9.0988×10^{-6}	1.99	8.0113×10^{-6}	2.00
2^{10}	1.7943×10^{-6}	2.00	2.8522×10^{-6}	2.00	2.2747×10^{-6}	1.99	2.0028×10^{-6}	1.99
2^{11}	4.4664×10^{-7}	1.99	7.1235×10^{-7}	2.00	5.6867×10^{-7}	1.99	5.0071×10^{-7}	1.99
2^{12}	1.1208×10^{-7}	-	1.7798×10^{-7}	-	1.4217×10^{-7}	-	1.2518×10^{-7}	-
	$\varepsilon = 2^{-1}$		$\varepsilon = 2^{-2}$		$\varepsilon = 2^{-4}$		$\varepsilon = 2^{-6}$	
	E_n	Ord	E_n	Ord	E_n	Ord	E_n	Ord
2^5	8.0580×10^{-4}	1.91	2.8396×10^{-3}	1.91	1.8411×10^{-2}	1.87	2.5405×10^{-2}	1.55
2^6	2.1384×10^{-4}	2.00	7.5103×10^{-4}	1.98	5.0284×10^{-3}	1.87	8.6260×10^{-3}	1.94
2^7	5.3389×10^{-5}	2.00	1.8918×10^{-4}	1.99	1.3690×10^{-3}	1.99	2.2443×10^{-3}	1.96
2^8	1.3343×10^{-5}	2.00	4.7545×10^{-5}	1.99	3.4442×10^{-4}	1.99	5.7294×10^{-4}	1.99
2^9	3.3354×10^{-6}	2.00	1.1891×10^{-5}	1.99	8.6242×10^{-5}	1.99	1.4382×10^{-4}	1.99
2^{10}	8.3385×10^{-7}	1.99	2.9731×10^{-6}	1.99	2.1569×10^{-5}	1.99	3.6007×10^{-5}	1.99
2^{11}	2.0847×10^{-7}	1.99	7.4330×10^{-7}	1.99	5.3941×10^{-6}	1.99	9.0035×10^{-6}	1.99
2^{12}	5.2119×10^{-8}	-	1.8582×10^{-7}	-	1.3485×10^{-6}	-	2.2511×10^{-6}	-
	$\varepsilon = 2^{-8}$		$\varepsilon = 2^{-10}$		$\varepsilon = 2^{-15}$		$\varepsilon = 2^{-20}$	
	E_n	Ord	E_n	Ord	E_n	Ord	E_n	Ord
2^5	2.7179×10^{-2}	1.38	3.1161×10^{-2}	1.05	3.2248×10^{-2}	0.90	3.256×10^{-2}	0.83
2^6	1.0409×10^{-2}	1.93	1.4997×10^{-2}	1.90	1.7256×10^{-2}	1.89	1.8217×10^{-2}	1.88
2^7	2.7271×10^{-3}	1.98	3.9998×10^{-3}	1.97	4.6439×10^{-3}	1.94	4.9220×10^{-3}	1.93
2^8	6.9017×10^{-4}	1.99	1.0173×10^{-3}	1.98	1.2033×10^{-3}	1.98	1.2901×10^{-3}	1.99
2^9	1.7311×10^{-4}	1.99	2.5733×10^{-4}	1.99	3.0342×10^{-4}	1.99	3.2443×10^{-4}	1.99
2^{10}	4.3391×10^{-5}	1.99	6.4406×10^{-5}	1.99	7.6080×10^{-5}	1.99	8.1369×10^{-5}	1.99
2^{11}	1.0850×10^{-5}	1.99	1.6106×10^{-5}	1.99	1.9026×10^{-5}	1.99	2.0349×10^{-5}	1.99
2^{12}	2.7126×10^{-6}	-	4.0275×10^{-6}	-	4.7576×10^{-6}	-	5.0882×10^{-6}	-
	$\varepsilon = 2^{-25}$		$\varepsilon = 2^{-30}$		$\varepsilon = 2^{-35}$		$\varepsilon = 2^{-40}$	

TABLE 1. The values of E_n, and Ord for the different values of N and ε for Liseikin mesh.

The notation remains consistent with that used in Example 1. Figure 4 illustrates the numerical solutions alongside their corresponding exact solutions, computed on the Liseikin mesh for three different values of the parameter ε. A detailed view of the numerical solutions within the boundary layer near $x = 0$ is provided in Figure 5, where each solution is obtained using a different mesh type. The maximum nodal errors E_N and the numerical rates of convergence Ord are presented in Tables 4, 5, and 6 for the Liseikin, Bakhvalov, and Shishkin meshes, respectively.

Bakhvalov mesh								
N	E_n	Ord	E_n	Ord	E_n	Ord	E_n	Ord
2^5	2.5490×10^{-3}	1.99	3.0112×10^{-3}	1.96	2.5191×10^{-2}	1.91	5.7739×10^{-2}	1.20
2^6	6.3767×10^{-4}	1.99	7.7194×10^{-4}	1.99	6.6834×10^{-3}	1.81	$2.506\,48 \times 10^{-2}$	1.93
2^7	1.5944×10^{-4}	1.99	1.9304×10^{-4}	1.99	1.9042×10^{-3}	1.95	6.5569×10^{-3}	1.55
2^8	3.9864×10^{-5}	1.99	4.8262×10^{-5}	1.99	4.8991×10^{-4}	1.99	2.2281×10^{-3}	1.90
2^9	9.9662×10^{-6}	1.99	1.2065×10^{-5}	1.99	1.2328×10^{-4}	1.99	5.9498×10^{-4}	1.95
2^{10}	2.4915×10^{-6}	1.99	3.0164×10^{-6}	1.99	3.0896×10^{-5}	1.99	1.5353×10^{-4}	1.99
2^{11}	6.2289×10^{-7}	1.99	7.5411×10^{-7}	1.99	7.7266×10^{-6}	1.99	3.8610×10^{-5}	1.99
2^{12}	1.5572×10^{-7}	-	1.8852×10^{-7}	-	1.9319×10^{-6}	-	9.6756×10^{-6}	-
	$\varepsilon = 2^{-1}$		$\varepsilon = 2^{-2}$		$\varepsilon = 2^{-4}$		$\varepsilon = 2^{-6}$	
	E_n	Ord	E_n	Ord	E_n	Ord	E_n	Ord
2^5	1.0756×10^{-1}	0.97	1.4009×10^{-1}	0.94	6.2242×10^{-2}	1.41	3.8858×10^{-3}	2.81
2^6	5.4720×10^{-2}	1.86	7.2751×10^{-2}	1.74	2.3338×10^{-2}	2.53	5.5359×10^{-4}	1.91
2^7	1.5008×10^{-2}	0.67	2.1679×10^{-2}	0.23	4.0185×10^{-3}	0.05	1.4663×10^{-4}	2.13
2^8	9.4212×10^{-3}	1.36	1.8407×10^{-2}	0.89	3.8598×10^{-3}	0.06	3.3293×10^{-5}	1.22
2^9	3.6570×10^{-3}	1.98	9.8904×10^{-3}	1.18	3.6782×10^{-3}	1.41	1.4200×10^{-5}	2.73
2^{10}	9.2228×10^{-4}	1.78	4.3487×10^{-3}	1.97	1.3755×10^{-3}	2.47	2.1373×10^{-6}	1.90
2^{11}	2.6817×10^{-4}	1.96	1.1095×10^{-3}	1.49	2.4747×10^{-4}	0.26	5.7202×10^{-7}	2.15
2^{12}	6.8892×10^{-5}	-	3.9300×10^{-4}	-	2.0637×10^{-4}	-	1.2825×10^{-7}	-
	$\varepsilon = 2^{-8}$		$\varepsilon = 2^{-10}$		$\varepsilon = 2^{-15}$		$\varepsilon = 2^{-20}$	
	E_n	Ord	E_n	Ord	E_n	Ord	E_n	Ord
2^5	3.9062×10^{-3}	2.81	3.9062×10^{-3}	2.81	3.9062×10^{-3}	2.81	3.9062×10^{-3}	2.81
2^6	5.5423×10^{-4}	1.91	5.5424×10^{-4}	1.91	5.5424×10^{-4}	1.91	5.5426×10^{-4}	1.91
2^7	1.4664×10^{-4}	2.13	1.4664×10^{-4}	2.13	1.4664×10^{-4}	2.13	1.4664×10^{-4}	2.13
2^8	3.3337×10^{-5}	1.12	3.3337×10^{-5}	1.12	3.3337×10^{-5}	1.12	3.3337×10^{-5}	1.12
2^9	1.5257×10^{-5}	2.81	1.5258×10^{-5}	2.81	1.5258×10^{-5}	2.81	1.5259×10^{-5}	2.81
2^{10}	2.1716×10^{-6}	1.92	2.1716×10^{-6}	1.92	2.1716×10^{-6}	1.92	2.1717×10^{-6}	1.92
2^{11}	5.7304×10^{-7}	2.13	5.7304×10^{-7}	2.13	5.7304×10^{-7}	2.13	5.7304×10^{-7}	2.13
2^{12}	1.3024×10^{-7}	-	1.3024×10^{-7}	-	1.3024×10^{-7}	-	1.3024×10^{-7}	-
	$\varepsilon = 2^{-25}$		$\varepsilon = 2^{-30}$		$\varepsilon = 2^{-35}$		$\varepsilon = 2^{-40}$	

TABLE 2. The values of E_n, and Ord for the different values of N and ε for Bakhvalov mesh.

The discussion of the numerical results. The theoretical results established in this paper were validated through two numerical examples. In Example 1, the exact solution is known, whereas in Example 2, the exact solution is unknown, necessitating the use of the double-mesh principle. To evaluate the performance of the proposed method, three types of layer-adapted meshes were employed: Liseikin, Bakhvalov, and Shishkin. The latter two were included for comparison, as they are classical meshes specifically designed for resolving exponential layers. The maximum nodal errors E_N and the numerical rates of convergence Ord were computed using standard methodologies appropriate for each mesh type and the availability of an exact solution. These results, summarized in the

Shishkin mesh								
N	E_n	Ord	E_n	Ord	E_n	Ord	E_n	Ord
2^5	/	/	7.6166×10^{-3}	3.07	6.0292×10^{-3}	3.58	6.2134×10^{-2}	2.32
2^6	/	/	1.5870×10^{-3}	2.21	9.6814×10^{-4}	3.61	1.8962×10^{-2}	2.80
2^7	/	/	4.7977×10^{-4}	-0.9	1.3813×10^{-4}	3.12	4.1701×10^{-3}	3.01
2^8	/	/	8.2834×10^{-4}	0.43	2.4027×10^{-5}	1.82	7.7288×10^{-4}	3.03
2^9	/	/	6.4399×10^{-4}	0.91	8.3868×10^{-6}	1.93	1.3510×10^{-4}	2.99
2^{10}	/	/	3.7673×10^{-4}	1.25	2.6815×10^{-6}	1.97	2.3202×10^{-5}	2.95
2^{11}	/	/	1.7806×10^{-4}	1.55	8.2123×10^{-7}	1.99	3.9593×10^{-6}	2.92
2^{12}	/	/	6.9220×10^{-5}	-	2.4527×10^{-7}	-	6.7347×10^{-7}	-
	$\varepsilon = 2^{-1}$		$\varepsilon = 2^{-2}$		$\varepsilon = 2^{-4}$		$\varepsilon = 2^{-6}$	
	E_n	Ord	E_n	Ord	E_n	Ord	E_n	Ord
2^5	1.3592×10^{-1}	1.16	1.6560×10^{-1}	0.80	1.0658×10^{-2}	1.89	1.0658×10^{-2}	1.89
2^6	7.4963×10^{-2}	1.52	1.1000×10^{-1}	0.87	4.0411×10^{-3}	1.97	4.0411×10^{-3}	1.97
2^7	3.2964×10^{-2}	2.07	6.8656×10^{-2}	1.06	1.3915×10^{-3}	1.98	1.3915×10^{-3}	1.98
2^8	1.0342×10^{-2}	2.57	3.7931×10^{-2}	1.41	4.5867×10^{-4}	1.99	4.5867×10^{-4}	1.99
2^9	2.3471×10^{-3}	2.81	1.6764×10^{-2}	1.95	1.4546×10^{-4}	1.99	1.4546×10^{-4}	1.99
2^{10}	4.4742×10^{-4}	2.87	5.3049×10^{-3}	2.46	4.4922×10^{-5}	1.99	4.4922×10^{-5}	1.99
2^{11}	8.0353×10^{-5}	2.86	1.2142×10^{-3}	2.72	1.3595×10^{-5}	1.99	1.3595×10^{-5}	1.99
2^{12}	1.4194×10^{-5}	-	2.3296×10^{-4}	-	4.0452×10^{-6}	-	4.0452×10^{-6}	-
	$\varepsilon = 2^{-8}$		$\varepsilon = 2^{-10}$		$\varepsilon = 2^{-15}$		$\varepsilon = 2^{-20}$	
	E_n	Ord	E_n	Ord	E_n	Ord	E_n	Ord
2^5	1.0658×10^{-2}	1.89	1.0658×10^{-2}	1.89	1.0658×10^{-2}	1.89	1.0659×10^{-2}	1.89
2^6	4.0411×10^{-3}	1.97	4.0411×10^{-3}	1.97	4.0411×10^{-3}	1.97	4.0411×10^{-3}	1.97
2^7	1.3915×10^{-3}	1.98	1.3915×10^{-3}	1.98	1.3915×10^{-3}	1.98	1.3918×10^{-3}	1.98
2^8	4.5867×10^{-4}	1.99	4.5867×10^{-4}	1.99	4.5868×10^{-4}	1.99	4.5867×10^{-4}	1.99
2^9	1.4546×10^{-4}	1.99	1.4546×10^{-4}	1.99	1.4546×10^{-4}	1.99	1.4546×10^{-4}	1.99
2^{10}	4.4922×10^{-5}	1.99	4.4922×10^{-5}	1.99	4.4923×10^{-5}	1.99	4.4933×10^{-5}	1.99
2^{11}	1.3595×10^{-5}	1.99	1.3595×10^{-5}	1.99	1.3595×10^{-5}	1.99	1.3601×10^{-5}	2.00
2^{12}	4.0452×10^{-6}	-	4.0452×10^{-6}	-	4.0452×10^{-6}	-	4.0452×10^{-6}	-
	$\varepsilon = 2^{-25}$		$\varepsilon = 2^{-30}$		$\varepsilon = 2^{-35}$		$\varepsilon = 2^{-40}$	

TABLE 3. The values of E_n, and Ord for the different values of N and ε for Shishkin mesh.

provided tables, confirm the ε-uniform second-order convergence of the method. Complementing the numerical data, Figures 2 and 4 illustrate the behavior of the numerical solutions. These plots clearly depict the formation of boundary layers near the endpoints $x = 0$ and $x = 1$. As expected, smaller values of ε result in steeper gradients, while larger values lead to smoother transitions. A key observation from these figures is that the numerical solution points are effectively distributed across the entire domain, adequately capturing both the layer and the outer regions. Furthermore, the detailed views of the layers (Figures 3 and 5) demonstrate the ability of different meshes to resolve the solution under the same perturbation parameter ε. All computations were performed on a desktop

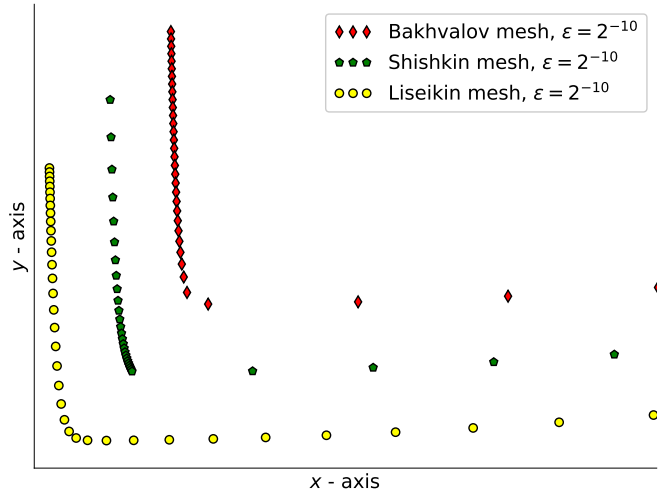

FIGURE 3. The layer near the endpoint $x = 0$.

computer equipped with an Intel® Core™ i7-12700 (20 cores) processor and 32 GiB of RAM. The algorithms were implemented in the Julia programming language, utilizing built-in linear solvers. In general, doubling the number of mesh points N increased the computation time by approximately a factor of four. However, in Example 2, a sharp increase in computational cost was observed for the Bakhvalov mesh at $N = 2^{10}$ and the Shishkin mesh at $N = 2^{12}$. This increased complexity is the reason for the fewer rows in the corresponding tables. While the values of E_N and Ord fell within expected theoretical bounds for most cases, some deviations were noted for the Bakhvalov mesh in Example 2. Most importantly, the parameters for the Liseikin mesh remained constant throughout all experiments, demonstrating its robustness. In contrast, the parameters for the Bakhvalov and Shishkin meshes required several manual adjustments to maintain stability across different values of N and ε.

This was one of the primary objectives when selecting the mesh. These points represent the values that were actually computed. The fact that the points are distributed evenly is important, as it demonstrates that the mesh is well-suited for the problem discussed in this paper. Furthermore, Figure 2 which presents the exact solutions alongside the numerical solutions shows that the error values are notably small, thereby confirming the proven order of convergence.

The detailed views provided in Figures 3 and 5 are particularly revealing. These figures focus on the numerical solutions within the boundary layer near the endpoint $x = 0$, computed for a fixed value of ε across different mesh types.

Liseikin grid								
N	E_n	Ord	E_n	Ord	E_n	Ord	E_n	Ord
2^5	3.6019×10^{-4}	1.97	8.5303×10^{-4}	1.99	3.9531×10^{-3}	1.99	2.1794×10^{-3}	1.92
2^6	9.1408×10^{-5}	1.98	2.1458×10^{-4}	1.99	9.9192×10^{-4}	1.99	2.1794×10^{-3}	1.98
2^7	2.3017×10^{-5}	1.95	5.3657×10^{-5}	1.99	2.4827×10^{-4}	1.99	1.4440×10^{-4}	1.99
2^8	5.7740×10^{-6}	2.00	1.3414×10^{-5}	2.00	6.2136×10^{-5}	1.99	3.6284×10^{-5}	1.99
2^9	1.4393×10^{-6}	2.11	3.3525×10^{-6}	2.00	1.5534×10^{-5}	2.00	9.0747×10^{-6}	2.00
2^{10}	3.3339×10^{-7}	2.00	8.3269×10^{-7}	2.09	3.8832×10^{-6}	2.00	2.2678×10^{-6}	2.01
2^{11}	8.3348×10^{-8}	2.00	1.9537×10^{-7}	2.00	9.6898×10^{-7}	1.87	5.6292×10^{-7}	1.96
2^{12}	2.0837×10^{-8}	-	4.8843×10^{-8}	-	2.6463×10^{-7}	-	1.4458×10^{-7}	-
	$\varepsilon = 2^{-1}$		$\varepsilon = 2^{-2}$		$\varepsilon = 2^{-4}$		$\varepsilon = 2^{-6}$	
	E_n	Ord	E_n	Ord	E_n	Ord	E_n	Ord
2^5	1.5123×10^{-2}	1.62	1.5123×10^{-2}	1.62	2.0703×10^{-2}	0.36	2.0493×10^{-2}	0,46
2^6	1.5123×10^{-2}	1.92	4.8869×10^{-3}	1.92	1.2203×10^{-2}	1.68	1.4877×10^{-2}	1.74
2^7	1.2870×10^{-3}	1.95	1.2870×10^{-3}	1.95	3.3924×10^{-3}	1.90	4.4450×10^{-3}	1.88
2^8	3.3184×10^{-4}	1.99	3.3184×10^{-4}	1.99	9.0631×10^{-4}	1.96	1.2022×10^{-3}	1.97
2^9	8.3202×10^{-5}	1.99	8.3202×10^{-5}	1.99	2.2838×10^{-4}	1.99	3.0482×10^{-4}	1.99
2^{10}	2.0815×10^{-5}	1.99	2.0815×10^{-5}	1.99	5.7210×10^{-5}	1.99	7.6598×10^{-5}	1.99
2^{11}	5.2040×10^{-6}	2.00	5.2040×10^{-6}	2.00	1.4316×10^{-5}	1.99	1.9162×10^{-5}	1.99
2^{12}	1.2977×10^{-6}	-	1.2977×10^{-6}	-	3.5780×10^{-6}	-	4.7915×10^{-6}	-
	$\varepsilon = 2^{-8}$		$\varepsilon = 2^{-10}$		$\varepsilon = 2^{-15}$		$\varepsilon = 2^{-20}$	
	E_n	Ord	E_n	Ord	E_n	Ord	E_n	Ord
2^5	2.0220×10^{-2}	0.36	2.0099×10^{-2}	0.33	2.0047×10^{-2}	0.32	2.0025×10^{-2}	0.31
2^6	1.5659×10^{-2}	1.68	1.5915×10^{-2}	1.66	1.6011×10^{-2}	1.65	1.6050×10^{-2}	1.65
2^7	4.8726×10^{-3}	1.90	5.0221×10^{-3}	1.91	5.0795×10^{-3}	1.91	5.1031×10^{-3}	1.91
2^8	1.3005×10^{-3}	1.96	1.3343×10^{-3}	1.96	1.3472×10^{-3}	1.95	1.3525×10^{-3}	1.95
2^9	3.3281×10^{-4}	1.99	3.4256×10^{-4}	1.99	3.4628×10^{-4}	1.99	3.4782×10^{-4}	1.99
2^{10}	8.3446×10^{-5}	1.99	8.5896×10^{-5}	1.99	8.6833×10^{-5}	1.99	8.7220×10^{-5}	1.99
2^{11}	2.0883×10^{-5}	1.99	2.1489×10^{-5}	1.99	2.1724×10^{-5}	1.99	2.1821×10^{-5}	1.80
2^{12}	5.2215×10^{-6}	-	5.3730×10^{-6}	-	5.4312×10^{-6}	-	6.2351×10^{-6}	-
	$\varepsilon = 2^{-25}$		$\varepsilon = 2^{-30}$		$\varepsilon = 2^{-35}$		$\varepsilon = 2^{-40}$	

TABLE 4. The values of E_n, and Ord for the different values of N and ε for Liseikin mesh.

In the plots corresponding to the Bakhvalov and Shishkin meshes, an abrupt transition between the fine and coarse regions of the grid is clearly visible, where the distance between adjacent mesh points changes rapidly. In contrast, the Liseikin mesh provides a remarkably smooth transition. Consequently, the points on the numerical solution graphics curves for the Liseikin mesh are more consistently spaced relative to one another than in the cases of the Bakhvalov or Shishkin meshes. The significance of these facts is that the points on the numerical solution graphics obtained using the Liseikin mesh are much closer to one another than those obtained with Bakhvalov or Shishkin meshes. This observation suggests why the results presented in the tables are achieved.

Bakhvalov mesh								
N	E_n	Ord	E_n	Ord	E_n	Ord	E_n	Ord
2^5	4.5049×10^{-5}	1.98	4.2025×10^{-4}	1.91	2.2214×10^{-3}	1.89	5.4659×10^{-3}	2.15
2^6	1.1292×10^{-5}	1.99	1.0687×10^{-4}	1.97	5.9547×10^{-4}	1.87	1.2287×10^{-3}	1.48
2^7	2.8358×10^{-6}	1.99	2.6843×10^{-5}	1.99	1.6220×10^{-4}	1.93	4.4047×10^{-4}	1.72
2^8	7.0910×10^{-7}	1.99	6.7159×10^{-6}	1.99	4.2481×10^{-5}	1.97	1.3353×10^{-4}	1.86
2^9	1.7735×10^{-7}	-	1.6797×10^{-6}	-	1.0790×10^{-5}	-	3.6622×10^{-5}	-
	$\varepsilon = 2^{-1}$		$\varepsilon = 2^{-2}$		$\varepsilon = 2^{-4}$		$\varepsilon = 2^{-6}$	
	E_n	Ord	E_n	Ord	E_n	Ord	E_n	Ord
2^5	7.9064×10^{-4}	2.73	9.2803×10^{-4}	2.91	9.9405×10^{-4}	2.98	9.9647×10^{-4}	2.99
2^6	1.1892×10^{-4}	1.87	1.2316×10^{-4}	1.91	1.2533×10^{-4}	1.93	1.2541×10^{-4}	1.93
2^7	3.2472×10^{-5}	2.17	3.2719×10^{-5}	2.18	3.2796×10^{-5}	2.18	3.2798×10^{-5}	2.18
2^8	7.1916×10^{-6}	2.00	7.2077×10^{-6}	1.88	7.2124×10^{-6}	1.10	7.2125×10^{-6}	1.05
2^9	1.7928×10^{-6}	-	1.9478×10^{-6}	-	3.3451×10^{-6}	-	3.4660×10^{-6}	-
	$\varepsilon = 2^{-8}$		$\varepsilon = 2^{-10}$		$\varepsilon = 2^{-15}$		$\varepsilon = 2^{-20}$	
	E_n	Ord	E_n	Ord	E_n	Ord	E_n	Ord
2^5	9.9654×10^{-4}	2.99	9.9654×10^{-4}	2.99	9.9654×10^{-4}	2.99	9.9654×10^{-4}	2.99
2^6	1.2541×10^{-4}	1.93	1.2541×10^{-4}	1.93	1.2541×10^{-4}	1.93	1.2541×10^{-4}	1.93
2^7	3.2798×10^{-5}	2.18	3.2798×10^{-5}	2.18	3.2798×10^{-5}	2.18	3.2798×10^{-5}	2.18
2^8	7.2125×10^{-6}	1.05	7.2125×10^{-6}	1.05	7.2125×10^{-6}	1.05	7.2125×10^{-6}	1.05
2^9	3.4702×10^{-6}	-	3.4703×10^{-6}	-	3.4703×10^{-6}	-	3.4703×10^{-6}	-
	$\varepsilon = 2^{-25}$		$\varepsilon = 2^{-30}$		$\varepsilon = 2^{-35}$		$\varepsilon = 2^{-40}$	

TABLE 5. The values of E_n, and Ord for the different values of N and ε for Bakhvalov mesh.

6. CONCLUSION

In this paper, we analyzed the numerical solution of a linear reaction-diffusion singularly perturbed problem. It is well known that the exact solution exhibits two boundary layers of exponential type near the endpoints $x = 0$ and $x = 1$.

While Bakhvalov- and Shishkin-type meshes are purpose-built to resolve such exponential layers, this study focused on the application of the Liseikin mesh. Although the Liseikin mesh is originally designed to address a wider class of layers, its application here demonstrates its effectiveness in resolving exponential layers as well. We have theoretically proven and numerically verified that the method is ε-uniformly convergent of order 2.

Furthermore, it is easy to notice that the analysis of this method is simpler than in the cases of using Bakhvalov or Shishkin meshes, precisely because the Liseikin mesh is constructed to resolve wider layers compared to standard exponential layers.

Finally, the theoretical findings were confirmed through two numerical examples.

Shishkin mesh								
N	E_n	Ord	E_n	Ord	E_n	Ord	E_n	Ord
2^5	1.0340×10^{-3}	2.34	1.1476×10^{-3}	1.99	2.5374×10^{-3}	1.93	$2.492\,52 \times 10^{-3}$	1.67
2^6	2.1566×10^{-3}	-1.4	4.1344×10^{-4}	2.00	9.4649×10^{-4}	1.98	$1.059\,26 \times 10^{-3}$	2.18
2^7	4.7473×10^{-3}	-1.4	1.4052×10^{-4}	2.00	3.2457×10^{-4}	1.99	3.2569×10^{-4}	1.98
2^8	8.7196×10^{-3}	-1.0	4.5841×10^{-5}	2.00	1.0646×10^{-4}	1.99	1.0722×10^{-4}	1.99
2^9	1.5008×10^{-2}	-0.9	1.4495×10^{-5}	2.00	3.3748×10^{-5}	1.99	3.4019×10^{-5}	1.99
2^{10}	/	/	4.4673×10^{-6}	-	1.0420×10^{-5}	1.99	1.0505×10^{-5}	1.99
2^{11}	/	/	/	/	3.1523×10^{-6}	-	3.1782×10^{-6}	-
	$\varepsilon = 2^{-1}$		$\varepsilon = 2^{-2}$		$\varepsilon = 2^{-4}$		$\varepsilon = 2^{-6}$	
	E_n	Ord	E_n	Ord	E_n	Ord	E_n	Ord
2^5	4.2790×10^{-3}	1.84	9.5806×10^{-3}	1.91	9.5820×10^{-3}	1.91	9.5820×10^{-3}	1.91
2^6	1.6672×10^{-3}	1.95	3.6065×10^{-3}	1.90	3.6070×10^{-3}	1.90	3.6070×10^{-3}	1.90
2^7	5.8277×10^{-4}	1.99	1.2934×10^{-3}	1.97	1.2936×10^{-3}	1.97	1.2936×10^{-3}	1.97
2^8	1.9120×10^{-4}	1.99	4.2849×10^{-4}	1.99	4.2856×10^{-4}	1.99	4.2856×10^{-4}	1.99
2^9	6.0562×10^{-5}	1.99	1.3614×10^{-4}	1.99	1.3616×10^{-4}	1.99	1.3616×10^{-4}	1.99
2^{10}	1.8709×10^{-5}	1.99	4.2111×10^{-5}	1.99	4.2118×10^{-5}	1.99	4.2118×10^{-5}	1.99
2^{11}	5.6613×10^{-6}	-	1.2741×10^{-5}	-	1.2743×10^{-5}	-	1.2743×10^{-5}	-
	$\varepsilon = 2^{-8}$		$\varepsilon = 2^{-10}$		$\varepsilon = 2^{-15}$		$\varepsilon = 2^{-20}$	
	E_n	Ord	E_n	Ord	E_n	Ord	E_n	Ord
2^5	9.5820×10^{-3}	1.91	9.5820×10^{-3}	1.91	9.5820×10^{-3}	1.91	9.5820×10^{-3}	1.91
2^6	3.6070×10^{-3}	1.90	3.6070×10^{-3}	1.90	3.6070×10^{-3}	1.90	3.6070×10^{-3}	1.90
2^7	1.2936×10^{-3}	1.97	1.2936×10^{-3}	1.97	1.2936×10^{-3}	1.97	1.2936×10^{-3}	1.97
2^8	4.2856×10^{-4}	1.99	4.2856×10^{-4}	1.99	4.2856×10^{-4}	1.99	4.2856×10^{-4}	1.99
2^9	1.3616×10^{-4}	1.99	1.3616×10^{-4}	1.99	1.3616×10^{-4}	1.99	1.3616×10^{-4}	1.99
2^{10}	4.2118×10^{-5}	1.99	4.2118×10^{-5}	1.99	4.2118×10^{-5}	1.99	4.2118×10^{-5}	1.99
2^{11}	1.2743×10^{-5}	-	1.2743×10^{-5}	-	1.2743×10^{-5}	-	1.2743×10^{-5}	-
	$\varepsilon = 2^{-25}$		$\varepsilon = 2^{-30}$		$\varepsilon = 2^{-35}$		$\varepsilon = 2^{-40}$	

TABLE 6. The values of E_n, and Ord for the different values of N and ε for Shishkin mesh.

ACKNOWLEDGMENTS

The author would like to thank the reviewers for their valuable comments, remarks, and suggestions, which have improved the quality of the paper.

REFERENCES

[1] N. S. Bakhvalov: *Towards optimization of methods for solving boundary value problems in the presence of boundary layers*. Zh. Vychisl. Mat. i Mat. Fiz.**9** (1969) pp. 841–859.

[2] E. P. Doolan, J. J. H. Miller and W. H. A. Schilders; *Uniform numerical methods for problems with initial and boundary layers*. Boole Press, Dublin, 1980. ISBN:9780906783023.

[3] D. Herceg, K. Surla, I. Radeka and H. Maličić; *Numerical Experiments with Different Schemes for a Singularly Perturbed Problem*, Novi Sad J. Math., Vol. 31, No. 1, 2001, pp. 93–101.

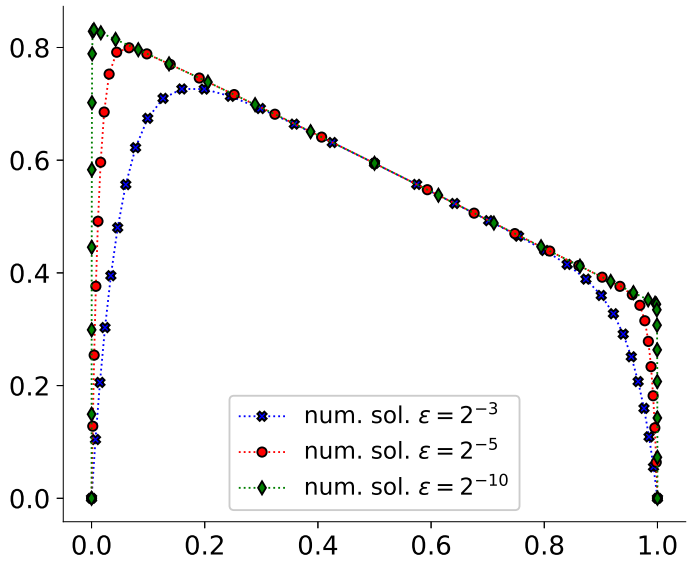

FIGURE 4. The numerical solutions for $N = 32$, and different values of ε on Liseikin mesh.

[4] P. A. Farrell, A. F. Hegarty, J. J. H. Miller, E. O'Riordan, and G. I. Shishkin, *Robust Computational Techniques for Boundary Layers*, Chapman&Hall/CRC, Boca Raton, Florida, USA, (2000).
[5] T. Linß, *Layer-adapted meshes for reaction-convection-diffusion problems*, Springer–Verlag Berlin Heidelberg, (2010).
[6] V. D. Liseikin, *Layer Resolving Grids and Transformations for Singular Perturbation Problems*, VSP BV, AH Zeist, The Netherlands, (2001).
[7] V. D. Liseikin, *Grid Generation for Problems with Boundary and Interior Layers*, Novosibirsk State University, Novosibirsk, Russia, (2018).
[8] V. D. Liseikin, *The Use of Special Transformations in The Numerical Solution of Boundary–Layer Problem*, U.S.S.R. Comput.Maths.Math.Phys., 30(1), (1990), pp. 43–53.
[9] V. D. Liseikin, S. Karasuljić, and V. I. Paasonen, *Numerical Grids and High–Order Schemes for Problems with Boundary and Interior Layers*, Novosibirsk State University, Novosibirsk, Russia, (2021).
[10] V. D. Liseikin and V. E. Petrenko, *The adaptive-invariant method for the numerical solution of problems with boundary and interior layers*, Novosibirsk: Vychislitel'nyj Tsentr SO AN SSSR, (1989).
[11] J. Lorenz, *Stability and monotonicity properties of stiff quasilinear boundary problems*, Zb.rad. Prir. Mat. Fak. Univ. Novom Sadu, Ser. Mat., 12, (1982), pp. 151–176.
[12] J. J. H. Miller, E. O'Riordan, and G. I. Shishkin, *Fitted Numerical Methods for Singular Perturbation Problems*, World Scientific Publishing Co.Pte.Ltd.Singapore, (1996).
[13] H. G. Roos, M. Stynes, M. and L. Tobiska, *Robust Numerical Methods for Singularly Perturbed Differential Equations*, Springer-Verlag Berlin Heidelberg, (2008).
[14] G. I. Shishkin, *Difference scheme on a nonuniform grid for a differential equation with small parameter multiplying the highest derivative*, 23(3), (1983), pp. 609–619.

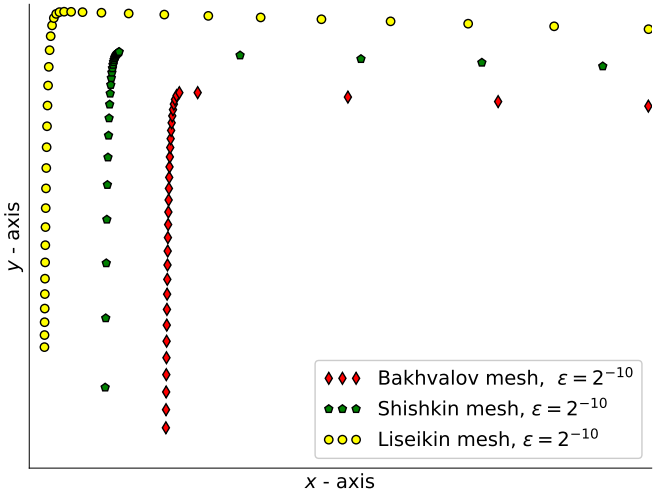

FIGURE 5. The layer near the endpoint $x = 0$.

[15] G.I. Shishkin, *Grid approximation of singularly perturbed parabolic equations with internal layers*, Sov. J. Numer. Anal. M.Russian Journal of Numerical Analysis and Mathematical Modelling, 3(5), (1988), pp. 393–408.

[16] R. Vulanović, *On a Numerical Solution of a Type of Singularly Perturbed Boundary Value Problem by Using a Special Discretization Mesh*, Novi Sad J. Math., 13, (1983), pp. 187–201.

SAMIR KARASULJIĆ
UNIVERSITY OF TUZLA,
FACULTY OF SCIENCES AND MATHEMATICS,
UNIVERZITETSKA 4, 75000 TUZLA, BOSNIA AND HERZEGOVINA
Email address: samir.karasuljic@gmail.com, samir.karasuljic@untz.ba

Received 26.11.2025
Revised 08.03.2026
Accepted 21.05.2026